



**HAL**  
open science

## Effects of aggregate size and alkali content on ASR expansion

Stéphane Multon, Martin Cyr, Alain Sellier, Paco Diederich, Laurent Petit

► **To cite this version:**

Stéphane Multon, Martin Cyr, Alain Sellier, Paco Diederich, Laurent Petit. Effects of aggregate size and alkali content on ASR expansion. *Cement and Concrete Research*, 2010, 40 (4), pp.508–516. 10.1016/j.cemconres.2009.08.002 . hal-01724664

**HAL Id: hal-01724664**

**<https://hal.insa-toulouse.fr/hal-01724664>**

Submitted on 23 Mar 2018

**HAL** is a multi-disciplinary open access archive for the deposit and dissemination of scientific research documents, whether they are published or not. The documents may come from teaching and research institutions in France or abroad, or from public or private research centers.

L'archive ouverte pluridisciplinaire **HAL**, est destinée au dépôt et à la diffusion de documents scientifiques de niveau recherche, publiés ou non, émanant des établissements d'enseignement et de recherche français ou étrangers, des laboratoires publics ou privés.

# 1 EFFECTS OF AGGREGATE SIZE AND ALKALI CONTENT ON ASR EXPANSION

2  
3 Stéphane Multon<sup>a</sup>, Martin Cyr<sup>a,\*</sup>, Alain Sellier<sup>a</sup>, Paco Diederich<sup>a</sup>, Laurent Petit<sup>b</sup>

4  
5 <sup>a</sup> Université de Toulouse; UPS, INSA; LMDC (Laboratoire Matériaux et Durabilité des  
6 Constructions); 135, avenue de Rangueil; F-31 077 TOULOUSE cedex 4, France.

7 <sup>b</sup> Electricité de France (EDF) - Recherche et Développement, Avenue des Renardières, 77818  
8 MORET SUR LOING Cedex, France

## 9 10 ABSTRACT

11 Attempts to model ASR expansion are usually limited by the difficulty of taking into account  
12 the heterogeneous nature and size range of reactive aggregates. This work is a part of an  
13 overall project aimed at developing models to predict the potential expansion of concrete  
14 containing alkali-reactive aggregates. The paper gives measurements in order to provide  
15 experimental data concerning the effect of particle size of an alkali-reactive siliceous  
16 limestone on mortar expansion. Results show that no expansion was measured on the mortars  
17 using small particles (under 80  $\mu\text{m}$ ) while the coarse particles (0.63-1.25 mm) gave the largest  
18 expansions (0.33%). When two sizes of aggregate were used, ASR-expansions decreased with  
19 the proportion of small particles. Models are proposed to study correlations between the  
20 measured expansions and parameters such as the size of aggregates and the alkali and reactive  
21 silica contents. The pessimum effect of reactive aggregate size is assessed and the  
22 consequences on accelerated laboratory tests are discussed.

23  
24 **Keywords:** Particle Size Distribution (B), Alkali-Aggregate Reaction (C), Alkalis (D),  
25 Modeling (E), pessimum of aggregate size

## 26 27 28 1 INTRODUCTION

29 Reassessment of structures (bridges and dams) damaged by the Alkali-Silica-Reaction is of  
30 prime importance for engineering structure owners. The gel volume formed by the chemical  
31 reaction can be used as input data to structural models [1]. One of the main difficulties is to  
32 assess the volume of this gel [2]. Microscopic models [3-7] could be one method of doing  
33 this. Such models should be able to predict the differences of expansions with the variation of  
34 all influential parameters (size of aggregate, silica content, alkali content, etc.) and have to be  
35 compared with experimental results.

---

\* Correspondence to: [cyr@insa-toulouse.fr](mailto:cyr@insa-toulouse.fr)

36 Numerous papers deal with the effect of particle size of reactive aggregates on the expansion  
37 due to ASR. Experiments have been performed on several types of aggregates. It seems that  
38 which aggregate size causes the highest ASR expansion depends on the nature and  
39 composition of the aggregate. Significant differences have been observed between rapid and  
40 slow alkali-reactive aggregates. Opal was one of the earliest and most widely used aggregates  
41 in laboratory studies of the size effect [8-12]. Investigations on the size effect have also been  
42 performed with different kinds of silica glass, fused silica, waste silica glass, andesite,  
43 siliceous limestone, quartzite, greywacke, chert, mylonite, flint and sandstone [13-18]. In  
44 spite of all these studies, it is difficult to generalize about the effect of the particle size of  
45 reactive aggregates, since conflicting results exist concerning the most damaging size that  
46 leads to the highest ASR expansion. All the results available in the literature were obtained  
47 using different experimental conditions and the effects due to coupling with other important  
48 parameters, such as Na/Si ratio, have been often neglected.

49 A few papers deal with the effect of size for reactive siliceous limestone [6,8,9,19]. This type  
50 of aggregate has been used in many damaged structures in France. Therefore, in order to test  
51 models to predict the potential expansion of concrete containing such alkali-reactive  
52 aggregates, tests have been performed to provide experimental data on the effect of particle  
53 size of an alkali-reactive siliceous limestone on mortar expansion. This paper presents the  
54 experimental results (expansion measurements performed over more than 500 days at 60°C)  
55 and gives data necessary for model development.

56 Sixteen mix-designs were studied and special attention was paid to the proportions of alkalis  
57 ( $\text{Na}_2\text{O}_{\text{eq}}$ ) in the mixtures and reactive silica in the aggregate. First, the paper presents the  
58 experimental conditions of the tests. Then, the measurements of ASR-expansions are  
59 presented in two parts: experiments on mortars containing one reactive size distribution (0-  
60 80  $\mu\text{m}$ , 80-160  $\mu\text{m}$ , 160-315  $\mu\text{m}$ , 315-630  $\mu\text{m}$ ; 630-1250  $\mu\text{m}$ , or 1250-2500  $\mu\text{m}$ ) and  
61 experiments on mortars containing mixes of two sizes of aggregate (0-80  $\mu\text{m}$  and 1250-  
62 3150  $\mu\text{m}$ ) with increasing 0-80  $\mu\text{m}$  reactive aggregate content. Finally, models are proposed  
63 to analyze the experimental results by studying correlations between the measured expansions  
64 and parameters such as the size of aggregates and the alkali and reactive silica contents. A  
65 time-dependent model allows the pessimum effect of reactive aggregate size to be assessed  
66 and its consequences on accelerated laboratory tests are discussed at the end.

67

68 **2 EXPERIMENTAL CONDITIONS**

69 **2.1 Materials**

70 The cement used was a standard CEM I 52,5R with a specific gravity of 3.1 and a specific  
71 surface area (Blaine) of 400 m<sup>2</sup>/kg. Its chemical composition is given in Table 1. The  
72 aggregates were crushed sands (jaw crusher): a non-reactive marble (NR) and a reactive  
73 siliceous limestone (R). The chemical composition of aggregates NR and R are given in Table  
74 1. The non-reactive marble was mainly composed of calcite. The reactive siliceous limestone  
75 contained mostly calcite and quartz, with traces of dolomite, feldspars and phyllosilicates. In  
76 order to control the particle size distribution of the aggregates in the mortars, the aggregate  
77 samples were divided into several particle size fractions: 0-80, 80-160, 160-315, 315-630,  
78 630-1250, 1250-2500 and 1250-3150 μm). Details of the aggregate combinations are given in  
79 2.3.

80  
81 **2.2 Methods**

82 Expansion was measured on mortar prisms (2x2x16cm) with a sand (1512 kg/m<sup>3</sup>) to cement  
83 (504 kg/m<sup>3</sup>) ratio of 3. The mortar prisms were demolded 24 hours after casting and were then  
84 kept in sealed bags at 20°C until 28 days. At 28 days of age, the prisms were stored at 60°C,  
85 after being placed on grids in watertight containers containing 20 mm of water (mortar bars  
86 were not in contact with water). Salt (K<sub>2</sub>SO<sub>4</sub>) was added to the water (above saturation) in  
87 order to maintain a relative humidity above 95% in the containers and to try to avoid  
88 condensation on the specimens. Expansion was measured using the scale micrometer method  
89 (specimens had shrinkage bolts at both ends). Each measurement was the mean of three  
90 values from three replicate specimens. Expansion measurements were performed after the  
91 containers and the prisms had been cooled for 24 hours at 20°C.

92 In order to reach specific Na/Si ratios, mixtures were adjusted to alkali contents (Na<sub>2</sub>O<sub>eq</sub>) of  
93 6.2, 8.1 and 9.9 kg of alkali per m<sup>3</sup> of mortar by adding NaOH in the mixing water. An alkali-  
94 free superplasticizer was used (0.5% dry matter of cement mass) in mortars to achieve a  
95 proper set in the molds.

96 For the first part, the water-cement ratio was 0.5. For the second part, the largest content  
97 (40%) of fine reactive particles (0-80 μm) absorbed too much water during the casting, the  
98 mortar was too dry to be cast with a ratio of 0.5 (even with a superplasticizer). Therefore, the  
99 water-cement ratio was increased to 0.6.

100

## 101 **2.3 Experimental program**

### 102 2.3.1 Size effect

103 The first experimentation presented in this paper concerns the study of size effects of the  
104 reactive siliceous limestone on ASR expansions. In this part, six particle size fractions were  
105 studied in mortars: 0-80 (mortar M1), 80-160 (M2), 160-315 (M3), 315-630 (M4), 630-1250  
106 (M5) and 1250-2500  $\mu\text{m}$  (M6). These mortars contained 8.1 kg of alkali per  $\text{m}^3$  of mortar. In  
107 order to obtain significant expansions with the aggregate studied in this paper, the content of  
108 reactive aggregate had to be at least 30%. The particle size distributions (Figure 1) were  
109 obtained by adding 30% of reactive aggregate of the six different fractions to 70% of a  
110 continuous size distribution (0-2500  $\mu\text{m}$ ) of non-reactive aggregate. Therefore, the particle  
111 size distributions were different for the six mortars. The effect of such differences in particle  
112 size distribution on the porosity of mortars was studied on mortars containing only non-  
113 reactive particles. Porosities measured using the AFPC-AFREM method [20] laid between  
114 17.3 and 18.2%. The differences did not appear to be significant compared to difference of  
115 1% which could be obtained during measurements made on three specimens of a given  
116 mortar.

117

### 118 2.3.2 Effect of fine reactive aggregate

119 For the second part of the experimentation, reactive particles of two sizes were used: 0-80  $\mu\text{m}$   
120 and 1250-3150  $\mu\text{m}$ , in mortars containing 6.2 and 9.9 kg of alkalis per  $\text{m}^3$  of mortar.  
121 Aggregates in all mortars had an equivalent particle size distribution and were composed of  
122 40% of 0-80  $\mu\text{m}$  particles, 30% of 315-630  $\mu\text{m}$  particles and 30% of 1250-3150  $\mu\text{m}$  particles.  
123 For the five reactive mortar mixtures studied, all the 315-630  $\mu\text{m}$  particles were non-reactive  
124 and all the 1250-3150  $\mu\text{m}$  particles were reactive. Only the nature of 0-80  $\mu\text{m}$  particles  
125 changed: mortars M7, M8, M9, M10 and M11 contained 0%, 10%, 20%, 30% and 40% of 0-  
126 80  $\mu\text{m}$  reactive aggregate and 40%, 30%, 20%, 10% and 0% of 0-80  $\mu\text{m}$  non-reactive  
127 aggregate, respectively. Therefore, mortars M7, M8, M9, M10 and M11 contained a total of  
128 30%, 40%, 50%, 60% and 70% of reactive particles, respectively. Moreover, measurements  
129 were performed on two reference mortars with only non-reactive aggregates (one for each  
130 alkali content).

131

## 132 **3 EXPERIMENTAL RESULTS**

### 133 **3.1 Size effect**

134 The experimental results are presented in Figures 2 and 3. The ASR-expansions presented in  
135 these figures were obtained by subtracting the expansion of the reference mortar (without  
136 reactive aggregate) from the total expansion, as already proposed by some authors [21-23].  
137 The long-term expansion of the reference mortars was 0.03%. The kinetics of the ASR-  
138 expansions measured for 500 days are given in Figure 2. After 500 days of exposure at 60°C  
139 and 95% R.H., mortars containing small reactive particles (0-80 and 80-160  $\mu\text{m}$ ) showed  
140 ASR-expansions lower than about 0.01% (Figure 3). ASR-expansions were measured for all  
141 the other mortars using particles larger than 160  $\mu\text{m}$ : 0.057% for 160-315  $\mu\text{m}$  reactive  
142 particles, 0.315% for 315-630  $\mu\text{m}$  particles, 0.328% for 630-1250  $\mu\text{m}$  particles and 0.267%  
143 for 1250-2500  $\mu\text{m}$  particles.

### 144 **3.2 Effect of fine reactive aggregate**

145 Measurements of the ASR-expansions were taken for more than 500 days for the two alkali  
146 contents (Figures 4 and 5). The ASR-expansions presented were obtained by subtracting the  
147 expansion of the reference mortar from the total expansion. The long-term expansions of the  
148 reference mortars were 0.02% and 0.03% for the low and the high alkali contents,  
149 respectively. For the two alkali contents, the mortars containing only the large reactive  
150 particles (M7) showed the largest ASR-expansions. Figure 6 shows the last ASR-expansion  
151 measured, related to the amount of fine reactive particles in the mortar mixtures. ASR-  
152 expansion decreased with the amount of fine reactive particles in the mortars: the more fine  
153 reactive particles the mortar contained, the smaller was the ASR-expansion.

## 155 **4 MODEL AND DISCUSSION**

156 The models presented in this section aim to improve the understanding of the experimental  
157 results obtained in the first part. The first model assesses the asymptotic expansion of mortars  
158 containing only one size (first set of experiments) or the mixture of two sizes (second set of  
159 experiments) of reactive aggregates. In order to integrate the dependence of swelling over  
160 time, a second model is then proposed. It will be shown that for a given duration of test and a  
161 given alkali content, the expansion is maximized for a specific range of aggregate size  
162 (pessimum effect). However, the time-dependent model does not consider the mixture of  
163 aggregates of different sizes for the moment. Finally, it should be noted that the fitted  
164 parameters supplied here are only applicable for the aggregate studied in this paper.

166

## 167 4.1 Asymptotic expansion model

### 168 4.1.1 Effects of aggregate size and alkali content on asymptotic expansion

169 For this reactive limestone, no ASR expansion was measured for small reactive particles (less  
170 than 160  $\mu\text{m}$ ). ASR-expansion appeared for particles having diameters greater than 160  $\mu\text{m}$   
171 (Figure 3). However, for the same content of reactive particles, the expansion was smaller for  
172 the 160-315  $\mu\text{m}$  reactive particles than for the 315-630  $\mu\text{m}$  reactive ones. The critical particle  
173 size that caused ASR-expansions was around 200 and 300  $\mu\text{m}$ . ASR-expansions increased  
174 with the size of reactive particles between 0 and 630  $\mu\text{m}$ . The ASR-expansion was very  
175 similar for the 315-630  $\mu\text{m}$  particles and for the 630-1250  $\mu\text{m}$  ones. Finally, the larger  
176 reactive particles showed lower expansions (Figure 3). This pessimum effect, which has  
177 already been observed for other reactive aggregates [10, 13], is assessed in the last part of this  
178 paper.

179 The expansion of the mortar is caused by the expansions of the ASR-gels. It can be assumed  
180 that this expansion is caused by the volume variation of the aggregate (in presence of gel). For  
181 the sake of simplicity, it is assumed in this paper that the mortar expansion due to ASR ( $\varepsilon_{ASR}$ )  
182 is proportional to the aggregate expansion (equation 1). For several sizes of reactive particles,  
183 the aggregate expansion is the sum of the expansions of all the reactive aggregates.

184

$$185 \quad \varepsilon_{ASR} = k \cdot \sum_{i=1}^{N_{rc}} \varphi_i^{agg} \varepsilon_i^{agg} \quad (1)$$

186 where  $\varepsilon_i^{agg}$  is the expansion of one reactive aggregate of class  $i$ ,  $\varphi_i^{agg}$  is the volume fraction of  
187 reactive aggregates of class  $i$  relative to the mortar volume (total volume of reactive aggregate  
188 of class  $i$  / total volume of the mortar),  $N_{rc}$  is the number of classes of reactive aggregates and  
189  $k$  is the fraction of expansion due to ASR related to the expansion of reactive aggregates.

190

191 The mortar expansion is assumed to be due to the aggregate expansion. If  $k=1$ , the mortar  
192 expansion is equal to the aggregate expansion (weighted by the volume fraction of reactive  
193 aggregates in the mortar). In reality,  $k$  has to be equal to or lower than 1, since the mortar  
194 expands less than the aggregate due to the mechanical effect of cement paste. The decrease of  
195 the value of the parameter  $k$  corresponds to the increase of the restraint of the cement paste on  
196 the aggregate. During ASR, when the aggregate swells, the cement paste is subjected to  
197 tensile stresses. Therefore, the effect of restraint is limited and the parameter  $k$  should not be  
198 too small.

199 During the formation of the ASR-gel, a part of the gel can migrate through the porosity close  
 200 to the aggregate without causing expansion. Therefore, the aggregate expansion for one  
 201 aggregate  $i$  can be described by equation 2.

202

$$203 \quad \varepsilon_i^{agg} = \frac{\langle V_i^{gel} - V_i^{poro} \rangle^+}{V_i^{agg}} \quad (2)$$

204 With:

205 -  $V_i^{agg}$ : the volume of one reactive particle,  $V_i^{agg} = \frac{4}{3}\pi \cdot R_i^3$ , where  $R_i$  is the radius of the  
 206 reactive particle.

207 -  $\langle X \rangle^+$ : the positive part of  $X$ : if  $X < 0$ ,  $\langle X \rangle^+ = 0$  otherwise  $\langle X \rangle^+ = X$

208 -  $V_i^{poro}$ : the volume of the porosity close to the reactive aggregate in which the ASR gel can  
 209 migrate without causing expansion. Assuming that the gel can migrate along the  
 210 same distance of the aggregate  $l_c$  whatever the size of the aggregate (simplifying  
 211 hypothesis), the volume of the porosity is given by equation 3, where  $\varphi^{void\_mortar}$  is  
 212 the porosity of the mortar.

$$213 \quad V_i^{poro} = \frac{4}{3}\pi \cdot ((R_i + l_c)^3 - R_i^3) \cdot \varphi^{void\_mortar} \quad (3)$$

214 -  $V_i^{gel}$ : the volume of ASR gel formed in only one reactive particle.

215

216 The volume of gel  $V_i^{gel}$  is considered as proportional to the alkali content and the reactive  
 217 aggregate volume, as defined by equation 4.

218

$$219 \quad V_i^{gel} = \varphi_i^{gel} \cdot V_i^{agg} \quad (4)$$

220 where  $\varphi_i^{gel}$  is the volume fraction of gel related to the particles of class  $i$ .  $\varphi_i^{gel}$  can be seen as  
 221 the volume of gel ( $m^3$ ) per  $m^3$  of aggregate: the higher the aggregate content, the higher the  
 222 amount of gel. It also implies that for high alkali content, more silica is attacked.

223

224 According to previous results [31] which showed that it was reasonable to use linear  
 225 relationships to express the expansions of mortars versus the alkali content and versus the  
 226 quantity of reactive particles, it can thus be assumed that  $\varphi_i^{gel}$  is proportional to:

227 - the alkali content of the mortar ( $AC$ ) minus a threshold of alkalis ( $AC_{th}$ ) under which no  
 228 expansion occurs. Usually, high alkali content implies deeper aggregate attack, and thus a  
 229 larger volume of gel per  $m^3$  of reactive aggregate. However, many papers [24-30] have shown  
 230 that, for low alkali contents (under a threshold lying between 3 and 5  $kg/m^3$ ), no expansion  
 231 occurs. The value of  $AC_{th}$  used in this work was 3.5  $kg/m^3$  [31].  $\varphi_{ref}^{gel}$  is a reference volume  
 232 fraction of gel fitted from tests on mortars containing  $AC_{ref}$  (alkali content of the mortar in the  
 233 first set of experiments - 8.1  $kg/m^3$ ).

234 - the volume fraction of the quantity of reactive particles of size  $i$  and the quantity of reactive  
 235 aggregate in the mortar (expressed as volume fractions  $\varphi_i^{agg}$  and  $\varphi_{tot}^{agg}$ ). In fact, the volume of  
 236 gel created by the reactive particles of one size depends on the content of the reactive  
 237 aggregates of this size compared to the content of all the reactive aggregates of the mortar. If  
 238 there are only large particles, all alkalis can react with these particles but when small particles  
 239 are added (as in the second set of experiments), the alkali content which reacts with the large  
 240 particles has to decrease. It can be assessed by equation 5 for a time corresponding to the end  
 241 of the tests.

242 From the above, the expression of the volume fraction of gel  $\varphi_i^{gel}$  can be given by equation 5.

$$243 \quad \varphi_i^{gel} = \varphi_{ref}^{gel} \frac{\langle AC - AC_{th} \rangle^+ \varphi_i^{agg}}{\langle AC_{ref} - AC_{th} \rangle^+ \varphi_{tot}^{agg}} \quad (5)$$

244 With:

245 -  $\varphi_{ref}^{gel}$ : reference volume fraction of gel fitted from tests with  $AC_{ref}$

246 -  $\varphi_i^{agg}$ : volume fraction of reactive aggregates of class  $i$  relative to the mortar

247 -  $\varphi_{tot}^{agg}$ : volume fraction of reactive aggregates (total: all classes) relative to the mortar

248 -  $AC$ : alkali content of the mortar

249 -  $AC_{th}$ : value of the threshold in alkali (taken equal to 3.5 kg/m<sup>3</sup>),

250 -  $AC_{ref}$ : alkali content of the mortar used to fit  $\varphi_{ref}^{gel}$  (8.1 kg/m<sup>3</sup>),

251

252 The combination of equations 1 to 5 for only one class of reactive particles (first set of  
 253 experiments) leads to the equation 6.

$$254 \quad \varepsilon_{ASR} = k \cdot \varphi_i^{agg} \cdot \left[ \left\langle \varphi_i^{gel} - \varphi^{void\_mortar} \cdot \left( \frac{(R_i + l_c)^3}{R_i^3} - 1 \right) \right\rangle^+ \right] \quad (6)$$

255 With  $\varphi_i^{gel} = \varphi_{ref}^{gel}$  since, for the first set of experiments,  $AC = AC_{ref} = 8.1$  kg/m<sup>3</sup> and  $\varphi_i^{agg} = \varphi_{tot}^{agg}$   
 256 (only one class of reactive particles).

257

258 In order to carry out this calculation, three parameters must be determined:  $l_c$ ,  $\varphi_{ref}^{gel}$  and  $k$ . In  
 259 this paper, several values for  $k$  between 0.1 and 1 are considered (for  $k = 0.1$ , the aggregate  
 260 swells 10 times more than the mortars), and  $l_c$  and  $\varphi_{ref}^{gel}$  are calculated to minimize the  
 261 deviation between the calculated value  $\varepsilon_{ASR}$  and the measured one. The value calculated using  
 262 equation 5 (which is a volumetric deformation) was divided by 3 in order to obtain linear  
 263 expansion (comparable to measured expansion on mortars).

264 The results of the calculations of the parameters are given in Table 2 and the calculated  
 265 expansions are plotted in Figure 7. Whatever the values of  $k$ , all the curves are quite similar,  
 266 so only one curve is plotted (named 'Asymptotic expansion model'). For the lower values of

267  $k$ , the values of  $l_c$  and  $\varphi_{ref}^{gel}$  are maximal (Table 2). The larger the cement paste restraint is, the  
268 larger the volume of ASR-gel must be to obtain significant expansion; and if there is a lot of  
269 gel,  $l_c$  has to be large to prevent expansion for the small reactive particles. For the values of  
270 the parameter  $k$  higher than 0.1, the value of the parameter  $l_c$  ranges between 11 and 91  $\mu\text{m}$ .  
271 Although the cement paste largely restrains the aggregate, this calculation can explain the  
272 increase of expansion with the size of the reactive particles.

273

274 To sum up, the model developed in this section assumes that the increase of ASR-expansion  
275 with the size of reactive particles can be explained by the effect of the porosity connected to  
276 the reactive aggregate. A porous crown of thickness  $l_c$  around the reactive aggregate, which is  
277 connected to the gel formation site, is defined. The volume of porosity to be filled around  
278 each particle of radius  $R_i$  before the expansion starts is given by equation 3. Figure 8 shows  
279 the total volume of porosity to be filled ( $V_i^{poro} \cdot N_i$ , in  $\text{m}^3$  per  $\text{m}^3$  of mortar) when considering  
280 the number of reactive aggregate of each size ( $N_i$ ). On the other hand, the volume of gel was  
281 computed according to equations 4 and 5, for which the volume of gel was considered as  
282 proportional to the alkali content and the aggregate volume. The expansion of an  
283 unconstrained mortar prism was then taken as the volumetric change of the aggregate due to  
284 the gel volume not contained in the porous crown (equations 1 and 2). This simple relation  
285 allows the final expansion to be plotted against the aggregate radius  $R_i$  and the alkali content.

286 The calculation can be generalized for different sizes of reactive aggregates and different  
287 alkali contents. Figure 9 shows the expansion of mortar prisms for ( $20 < R < 1000 \mu\text{m}$ ) and ( $3$   
288  $< AC < 10 \text{ kg/m}^3$ ). It can be seen that expansion increases linearly with the alkali content and  
289 non-linearly with the aggregate diameter. It could be concluded, abusively, from this figure  
290 that large aggregates and large alkali contents should lead to the highest expansion amplitude.  
291 However, even if a large aggregate presents a large expansion in this graph, a long test  
292 duration is needed in reality to obtain the final expansion amplitude, due to the long diffusion  
293 time for alkalis to reach the center of the particle (the porosity of this aggregate is less than  
294 1%). In contrast, for small aggregates, alkali ingress is faster and the reaction occurs rapidly,  
295 but the porous crown delays the expansion.

296 A pessimum size should exist for which the expansion is maximum for a given duration of  
297 test. This pessimum is obtained when the size of the aggregate is large enough to fill the  
298 connected porosity and the aggregate is completely attacked by the alkalis (while the larger

299 sizes are not). In order to gain a better understanding of these phenomena, a time-dependent  
300 expansion model is proposed in section 4.2.

301

#### 302 4.1.2 Effect of fine reactive aggregate on asymptotic expansion

303 For mortars containing two sizes of reactive particles, the larger the content of reactive  
304 aggregate was, the smaller were the ASR-expansions (Figure 6). In fact, the increase of the  
305 proportion of reactive aggregate was due to the increase of the smallest reactive particles (0-  
306 80  $\mu\text{m}$ ), while the proportion of the largest reactive particles (1250-3150  $\mu\text{m}$ ) was the same.  
307 The previous part showed that the smallest reactive particles did not cause expansion, but the  
308 largest ones expanded greatly. As the content of large particles was the same for all the five  
309 mortars (for one alkali content), expansions could be expected to be similar. However, the  
310 experimentation showed that the expansion decreased with increasing content of the small  
311 reactive particles. This effect has already been shown on concrete [32] and can sometimes be  
312 explained by the consumption of the alkalis by the small reactive particles. When aggregate  
313 powders are dispersed in a cement paste they release silica, resulting in a lowering of the  
314 Ca/Si ratio in C-S-H. It has been established that the ability of these low Ca/Si C-S-H to fix  
315 alkalis is enhanced. The depletion of free alkalis lowers the pH of the pore solution and,  
316 consequently, reduces the attack of reactive aggregates. Finally the expansion is reduced or  
317 suppressed. However, it should be noted that this explanation is not satisfactory in all cases:  
318 some alkali-releasing mineral admixtures can inhibit the reaction, or sometimes only retard it  
319 (e.g. high alkali fly ashes).

320

321 Calculations were performed using equations 1 to 5 for the two alkali contents and the two  
322 size classes of the second set of experiments, without any supplementary fitting. Figure 10  
323 gives the measured expansions versus the expansions assessed with the model with the  
324 parameters determined for  $k=1$  in the previous part (Table 2). As shown in Figure 10, the  
325 model gives values not too far from the measured expansions. The mean deviation between  
326 calculated and measured expansions is about 18%. It can be partly explained by the deviation  
327 between the model and the measurements for the largest particle for the parameter determined  
328 in the previous part. The value calculated for the largest particle was about 30% higher than  
329 the measurement (Figure 7). The overestimation of the expansion of coarse particles thus  
330 leads to an overestimate of the expansions of mortars containing mixtures of fine and coarse  
331 aggregates.

332 The model uses only proportionality between the parameters of volume of gel, alkali content  
 333 and reactive aggregate content. It appears to be efficient for assessing ASR-expansions in this  
 334 case for which mix designs and environmental conditions are perfectly known.

335

#### 336 **4.2 Time-dependent expansion model**

337 In order to improve the model, it is decided to use a time-dependent model which allows us to  
 338 (take into account) or (explain) the pessimum effect of coarse aggregates. A simplified  
 339 diffusion model is chosen, which does not consider the mixture of aggregates of different  
 340 sizes.

341 The simplest way to introduce the time effect in the previous model is to model the alkali  
 342 ingress kinetics through a simple phenomenological function. For experimental and physical  
 343 reasons, a square root function of the time is proposed [3]. The thickness of alkali penetration  
 344 from the paste to the center of the aggregate is thus given by equation 7.

$$345 \quad x(t) = R_{ref} \sqrt{\frac{t}{t_{ref}}} \quad (7)$$

346 With:

347  $x(t)$ : thickness of alkali penetration at a time  $t$ , from the paste to the center of the aggregate

348  $R_{ref}$ : radius of the aggregate used in the mortar for which the reference time  $t_{ref}$  is fitted

349  $t_{ref}$ : time necessary for alkali to reach the center of the aggregate of radius  $R_{ref}$ , fitted on  
 350 experimental results such as  $x(t_{ref}) = R_{ref}$ . In our case,  $t_{ref}$  was fitted using the radius  
 351  $R_{ref} = 236 \mu\text{m}$  (mortar M4 – size of aggregate: 315-630  $\mu\text{m}$ ). It was assumed that the  
 352 time necessary for alkali to reach the center of the aggregate of radius  $R_{ref} = 236 \mu\text{m}$   
 353 was 170 days (beginning of the asymptotic swelling of Mortar M4, as seen on Figure  
 354 2).

355  $t$ : duration of test

356

357 For a given duration  $t$ , the volume fraction of an aggregate of radius  $R_i$  affected by the  
 358 reaction is then given by equation 8.

359

$$360 \quad f(t) = \phi_i^{asr-agg}(t) = \frac{R_i^3 - \left( \langle R_i - x(t) \rangle^+ \right)^3}{R_i^3} \quad (8)$$

361

362 The combination of equations 1 to 5 and 7-8 for only one class of reactive particles leads to  
 363 the time-dependent model given by equation 9.

364

$$\begin{aligned}
\varepsilon_{ASR}(t) &= k \cdot \varphi_i^{agg} \cdot \varepsilon_i^{agg}(t) \\
365 \quad &= k \cdot \varphi_i^{agg} \cdot \frac{\langle V_i^{gel} \cdot f(t) - V_i^{poro} \rangle^+}{V_i^{agg}} \\
&= k \cdot \varphi_i^{agg} \cdot \left[ \left\langle \varphi_i^{gel} \cdot f(t) - \varphi^{void\_mortar} \cdot \left( \frac{(R_i + l_c)^3}{R_i^3} - 1 \right) \right\rangle^+ \right]
\end{aligned} \tag{9}$$

366 With  $\varphi_i^{gel} = \varphi_{ref}^{gel}$  (equation 5) since, for the first set of experiments,  $AC = AC_{ref} = 8.1 \text{ kg/m}^3$   
367 and  $\varphi_i^{agg} = \varphi_{tot}^{agg}$  (only one class of reactive particles).

368

369 In fact, in order to model the alkali consumption in a mixture, it is necessary to consider  
370 explicitly the decrease of the alkali content in the mortar due to the simultaneous consumption  
371 by all aggregates of different sizes. This phenomenon is a problem of coupled diffusion, too  
372 hard to be considered in a simple “summary model”. It is treated in detail in other works still  
373 in progress (and also in works such as Poyet et al. [6]).

374

375 Figure 7 compares the ASR-expansion of mortars containing one size of reactive particles  
376 (M1 to M6) with the asymptotic expansion model (section 4.1) and the time-dependent model  
377 developed in this section. It is observed that the time-dependent model represents the  
378 variation of the experimental data well, without any supplementary fitting of the parameters  
379 (except  $l_c$  and  $\varphi_{ref}^{gel}$  calculated from the first model).

380 Figure 11 generalizes the calculations of the expansion for various alkali contents (AC) and  
381 aggregate sizes (R) for test durations of 50 and 500 days. It shows that, for a sufficient  
382 amount of alkali, the dependence of the expansion on the aggregate size can be seen as a  
383 pessimum effect. For these simulations, the expansion at 50 days is maximal for a reactive  
384 aggregate radius around 200-250  $\mu\text{m}$ . This maximal expansion depends on the alkali content;  
385 it moves to 350  $\mu\text{m}$  if alkali content is close to 6  $\text{kg/m}^3$ . After longer times, the pessimum size  
386 increases (500-600  $\mu\text{m}$ ), since the alkali has had time to progress inside the aggregate.

387 Figure 12 gives the expansion curves for test durations up to 500 days and several aggregate  
388 radii, the alkali content being 8.1  $\text{kg/m}^3$ . This Figure shows that expansion curves are  
389 stabilized only for aggregates having radii of less than around 300  $\mu\text{m}$ .

390

### 391 **4.3 A synthesis of the part model and discussion**

392 The asymptotic expansion and time dependent models summarize the main experimental  
393 observations given in the previous sections. They allow some important phenomena linked to  
394 the size of reactive aggregate to be interpreted easily. Firstly, the decrease of expansion for

395 small aggregates is interpreted through the porous crown effect. Secondly, the slower  
396 expansion rate for large aggregates is explained using the alkali ingress kinetics.

397 It is interesting to note that the understanding of the pessimum effect of reactive aggregate  
398 size can be useful when fixing the parameters of accelerated laboratory tests. The model  
399 highlights the possibility of maximizing expansion, and consequently minimizing the test  
400 duration, by appropriate choices of both the alkali content and the aggregate size. This size  
401 must be sufficient to attenuate the connected porosity effect without making the duration of  
402 the test too long.

403 A direct application of this interpretation could be an original procedure aimed at minimizing  
404 the accelerated expansion test duration. For example, the authors are currently working on  
405 such a test clarification: it consists in extracting aggregates from an affected concrete,  
406 crushing them, and keeping only crushed particles of a given size. The mortars made with  
407 these aggregates (and an addition of alkalis) allow the potential for residual expansion of the  
408 concrete to be evaluated indirectly in the shortest possible time. Of course, this type of test  
409 must be combined with a particular model allowing the residual potential of the uncrushed  
410 aggregate in the concrete to be evaluated. Research is still in progress concerning this last  
411 topic.

412

## 413 **5 CONCLUSION**

414 This paper has presented the experimental measurements performed on 16 different mix-  
415 designs containing reactive siliceous limestone with special attention being paid to the  
416 proportions of alkalis ( $\text{Na}_2\text{O}_{\text{eq}}$ ) and reactive silica in the mixtures. It has been shown that:

417 - small reactive particles (under about 160  $\mu\text{m}$ ) do not cause expansion while coarse particles  
418 (0.63-1.25 mm) show the largest expansion (0.33%).

419 - ASR-expansion decreases with the amount of small particles when the mortars contain two  
420 sizes of aggregates (0-80 and 1250-3150  $\mu\text{m}$ ).

421

422 A first model shows that these results can be explained by the migration of ASR-gel in the  
423 porosity very close the reactive aggregate (less than 10  $\mu\text{m}$ ). The volume fraction of gel with  
424 respect to reactive aggregate has been considered as proportional to the alkali content of the  
425 mortar minus a threshold alkali content and to the proportion of reactive aggregates of each  
426 size compared to the content of all the reactive aggregates in the mortar. With these  
427 assumptions, the model predicts the expansions of the mortars containing two sizes of reactive  
428 aggregates.

429 In a second model, a time dependence of the expansion was introduced. It has been shown  
430 that, for a given duration of test and a given alkali content, the expansion is maximized for a  
431 specific range of aggregate size, which can be seen as a pessimum effect.

432

433 This approach allows a better understanding of the effects of aggregate size and alkali content  
434 on the expansion of mortars. It could also be useful for fixing the parameters of accelerated  
435 laboratory tests (maximizing expansion and minimizing duration of test). These tests and  
436 models will be used as a basis for the development of future models to assess the potential  
437 expansion of concrete containing alkali-reactive aggregates.

438

439

#### 440 **ACKNOWLEDGEMENTS**

441 The authors are grateful to EDF for supporting this work.

442

#### 443 **REFERENCES**

- 444 [1] B. Capra, A. Sellier, Orthotropic modelling of alkali-aggregate reaction in concrete  
445 structures: numerical simulations, *Mechanics of Materials* 35 (8) (2003) 817-830.
- 446 [2] A. Sellier, E. Bourdarot, S. Multon, M. Cyr, E. Grimal, 2007, Assessment of the  
447 residual expansion for expertise of structures affected by AAR, 10<sup>th</sup> International  
448 Conference on Alkali-Aggregate Reaction, Broekmans M.A.T.M. and Wigum B.J.  
449 (Eds), Trondheim, Norway, 2008, pp.1004-1013.
- 450 [3] Y. Furusawa, H. Ohga, T. Uomoto, An analytical study concerning prediction of  
451 concrete expansion due to Alkali-Silica Reaction, 3<sup>rd</sup> CANMET/ACI International  
452 Conference on Durability of Concrete, Nice, France, 1994, pp.757-779.
- 453 [4] A. Sellier, J.-P. Bournazel, A. Mébarki, Modelling the alkali aggregate reaction within a  
454 probabilistic frame-work, 10<sup>th</sup> International Conference on Alkali-Aggregate Reaction,  
455 Shayan A. (Ed), Melbourne, Australia, 1996, pp.694-701.
- 456 [5] Z.P. Bazant, A. Steffens, Mathematical model for kinetics of alkali silica reaction in  
457 concrete, *Cement and Concrete Research* 30 (3) (2000) 419-428.
- 458 [6] S. Poyet, A. Sellier, B. Capra, G. Foray, J.-M. Torrenti, H. Cognon, E. Bourdarot,  
459 Chemical modelling of Alkali Silica reaction: Influence of the reactive aggregate size  
460 distribution, *Materials and Structures* 40 (2) (2007) 229–239.
- 461 [7] A. Suwito, W. Jin, Y. Xi, C. Meyer, A mathematical model for the pessimum effect of  
462 ASR in concrete, *Concrete Science and Engineering* 4 (13) (2002) 23-34.
- 463 [8] D. McConnell, R.C. Mielenz, W.Y. Holland, K.T. Greene, Cement-aggregate reaction  
464 in concrete, *Journal of the American Concrete Institute, Proceedings* Vol.44, No.2,  
465 1947, pp.93-128.
- 466 [9] T.M. Kelly, L. Schuman, F.B. Hornibrook, A study of alkali-silica reactivity by means  
467 of mortar bar expansions, *Journal of the American Concrete Institute, Proceedings*  
468 Vol.45, No.1, 1948, pp.57-80.
- 469 [10] S. Diamond, N. Thaulow, A study of expansion due to alkali-silica reaction as  
470 conditioned by the grain size of the reactive aggregate, *Cement and Concrete Research*  
471 4 (4) (1974) 591-607.

- 472 [11] D.W. Hobbs, W.A. Gutteridge, Particle size of aggregate and its influence upon the  
473 expansion caused by the alkali-silica reaction, Magazine of Concrete research 31 (109)  
474 (1979) 235-242.
- 475 [12] M. Kawamura, K. Takemoto, S. Hasaba, Application of quantitative EDXA analyses  
476 and microhardness measurements to the study of alkali-silica reaction mechanisms, 6<sup>th</sup>  
477 International Conference of Alkalies in Concrete, Idorn G.M. and Rostam S. (Eds),  
478 Copenhagen, Denmark, 1983, pp.167-174.
- 479 [13] X. Zhang, G.W. Groves, The alkali-silica reaction in OPC/silica glass mortar with  
480 particular reference to pessimum effects, Advances in Cement Research, 3 (9) (1990) 9-  
481 13.
- 482 [14] L. Hasni, Y. Gallias, M. Salomon, Appréciation des risques d'alcali- réaction dans les  
483 bétons de sable, Rapport de recherche n°41020, Centre Expérimental de Recherches et  
484 d'Etudes du Bâtiment et des Travaux Publics (CEBTP), St-Rémy- lès-Chevreuses, 1993,  
485 53p.
- 486 [15] B.J. Wigum, W.J. French, Sequential examination of slowly expanding alkali-reactive  
487 aggregates in accelerated mortar bar testing, Magazine of Concrete research 48 (177)  
488 (1996) 281-292.
- 489 [16] C. Zhang, A. Wang, M. Tang, B. Wu, N. Zhang, Influence of aggregate size and  
490 aggregate size grading on ASR expansion, Cement and Concrete Research 29 (9) (1999)  
491 1393-1396.
- 492 [17] T. Kuroda, S. Inoue, A. Yoshino, S. Nishibayashi, Effects of particle size, grading and  
493 content of reactive aggregate on ASR expansion of mortars subjected to autoclave  
494 method, 12<sup>th</sup> International Conference on Alkali-Aggregate Reaction in Concrete, Tang  
495 M. and Deng M. (Eds), Beijing, China, 2004, pp.736-743.
- 496 [18] K. Ramyar, A. Topal, O. Andic, Effects of aggregate size and angularity on alkali-silica  
497 reaction, Cement and Concrete Research 35 (11) (2005) 2165-2169.
- 498 [19] M. Moisson, M. Cyr, E. Ringot, A. Carles-Gibergues, Efficiency of reactive aggregate  
499 powder in controlling the expansion of concrete affected by alkali-silica reaction (ASR),  
500 12<sup>th</sup> International Conference on Alkali-Aggregate Reaction in Concrete, Tang M. and  
501 Deng M. (Eds), Beijing, China, 2004, pp.617-624.
- 502 [20] AFPC–AFREM (Association Française Pour la Construction – Association Française de  
503 Recherche et Essais sur les Matériaux de construction), Durabilité des bétons. Méthodes  
504 recommandées pour la mesure des grandeurs associées à la durabilité. Mesure de la  
505 masse volumique apparente et de la porosité accessible à l'eau. Compte-Rendu des  
506 Journées Techniques, Toulouse, 11-12 December 1997, pp.121–124.
- 507 [21] T.N. Jones, A.B. Poole, Alkali-silica reaction in several U.K. concretes: the effect of  
508 temperature and humidity on expansion, and the significance of ettringite development,  
509 7<sup>th</sup> International Conference on Alkali-Aggregate Reaction in Concrete, Grattan-Bellew  
510 P.E. (Ed), Ottawa, Canada, 1986, pp.446-450.
- 511 [22] P.K. Mukherjee, J.A. Bickley, Performance of glass as concrete aggregates, 7<sup>th</sup>  
512 International Conference on Alkali-Aggregate Reaction in Concrete, Grattan-Bellew  
513 P.E. (Ed), Ottawa, Canada, 1986, pp.36-42.
- 514 [23] A. Carles-Gibergues, M. Cyr, Interpretation of expansion curves of concrete subjected  
515 to accelerated alkali-aggregate reaction (AAR) tests, Cement and Concrete Research 32  
516 (5) (2002) 691-700.
- 517 [24] Kodama K., Nishino T., Observation around the cracked region due to alkali-aggregate  
518 reaction by analytical electron microscope, 7<sup>th</sup> International Conference on Alkali-  
519 Aggregate Reaction in Concrete, Grattan-Bellew P.E. (Editor), Ottawa, Canada, 1986,  
520 pp.398-402.

- 521 [25] Kennerley R.A., St John D.A., Smith L.H., A review of thirty years of investigation of  
522 the alkali-aggregate reaction in New Zealand, 5<sup>th</sup> International Conference on Alkali-  
523 Aggregate Reaction in Concrete, National Building Research Institute of the CSIR  
524 (Editor), Cape Town, South Africa, 1981, S252/12, 9p.
- 525 [26] Oberholster R.E., Alkali reactivity of siliceous rock aggregates: diagnosis of the  
526 reaction, testing of cement and aggregate and prescription of preventive measures, 6<sup>th</sup>  
527 International Conference on Alkali-Aggregate Reaction in Concrete, Idorn G.M. and  
528 Rostam S. (Editors), Copenhagen, Denmark, 1983, pp.419-433.
- 529 [27] Hobbs D.W., Alkali-silica reaction in concrete, Thomas Telford, London, 1988.
- 530 [28] Rogers C.A., Hooton R.D., Reduction in mortar and concrete expansion with reactive  
531 aggregates due to alkali leaching, Cement, Concrete and Aggregates, 13 (1) (1991) 42-  
532 49.
- 533 [29] Thomas M.D.A., Blackwell B.Q., Nixon P.J., Estimating the alkali contribution from fly  
534 ash to expansion due to alkali-aggregate reaction in concrete, Magazine of Concrete  
535 Research, 48 (177) (1996) 251-264.
- 536 [30] Shehata M.H., Thomas M.D.A., The effect of fly ash composition on the expansion of  
537 concrete due to alkali-silica reaction, Cement and Concrete Research, 30 (7) (2000)  
538 1063-1072.
- 539 [31] S. Multon, M. Cyr, A. Sellier, N. Leklou, L. Petit, Coupled effects of aggregate size and  
540 alkali content on ASR expansion, Cement and Concrete Research 38 (3) (2008) 350-  
541 359.
- 542 [32] J.S. Guédon-Dubied, G. Cadoret, V. Durieux, F. Martineau, P. Fasseu, V. van  
543 Overbecke, Study on Tournai limestone in Antoing Cimescaut Quarry. Petrological,  
544 chemical and alkali reactivity approach, 11<sup>th</sup> International Conference on Alkali-  
545 Aggregate Reaction in Concrete, Bérubé M.A. Fournier B. Durand B. (Eds), Quebec  
546 City, Canada, 2000, pp.335-344.  
547  
548  
549

- 550 Notation:
- 551  $\varepsilon_{ASR}$ : expansion of mortar due to ASR
- 552  $\varepsilon_i^{agg}$ : expansion of one reactive aggregate of class i
- 553  $N_{rc}$ : number of classes of reactive aggregates
- 554  $k$ : fraction of expansion due to ASR related to the expansion of reactive aggregates
- 555  $l_c$ : distance of migration of the gel from the periphery of the aggregate
- 556  $\phi_i^{agg}$ : volume fraction of reactive aggregates of class i relative to the mortar
- 557  $\phi_{tot}^{agg}$ : volume fraction of reactive aggregates (total: all classes) relative to the mortar
- 558  $\phi_i^{gel}$ : volume fraction of gel related to the particles of class i ( $\phi_i^{gel} = V_i^{gel} / V_i^{agg}$ )
- 559  $\phi_{ref}^{gel}$ : reference volume fraction of gel fitted from tests with  $AC_{ref}$
- 560  $\phi^{void\_mortar}$ : porosity of the mortar
- 561  $V_i^{gel}$ : volume of ASR gel formed in only one reactive particle of class i
- 562  $V_i^{poro}$ : volume of the porosity close to a reactive aggregate of class i, from which ASR
- 563 gel can migrate without causing expansion
- 564  $V_i^{agg}$ : volume of one reactive particle of class i
- 565  $R_i$ : mean radius of reactive particle of class i
- 566  $AC$ : alkali content of the mortar
- 567  $AC_{th}$ : value of the threshold in alkali (taken equal to 3.5 kg/m<sup>3</sup>),
- 568  $AC_{ref}$ : alkali content of the mortar used to fit  $\phi_{ref}^{gel}$  (8.1 kg/m<sup>3</sup>),
- 569  $x(t)$ : thickness of alkali penetration at a time  $t$ , from the paste to the center of the aggregate
- 570  $R_{ref}$ : radius of the aggregate used in the mortar for which the reference time  $t_{ref}$  is fitted
- 571  $t_{ref}$ : time necessary for alkali to reach the center of the aggregate of radius  $R_{ref}$ , fitted on
- 572 experimental results such as  $x(t_{ref}) = R_{ref}$
- 573  $t$ : duration of test
- 574  $\phi_i^{asr-agg}(t)$ : volume fraction of an aggregate of class i affected by ASR at time  $t$
- 575
- 576
- 577
- 578

Table 1 - Chemical composition of cement and aggregates (% by mass).

	SiO <sub>2</sub>	Al <sub>2</sub> O <sub>3</sub>	Fe <sub>2</sub> O <sub>3</sub>	CaO	MgO	Na <sub>2</sub> O	K <sub>2</sub> O	Na <sub>2</sub> O <sub>eq</sub>	SO <sub>3</sub>	LOI
Cement	20.1	5.6	2.0	62.5	3.1	0.2	0.9	0.8	3.2	1.7
Non-reactive marble	-	-	-	54.4	0.5	0.001	-	-	0.01	43.0
Reactive siliceous limestone (1.25-3.15 mm)	20.0	1.3	0.6	40.6	1.2	0.4	0.4	0.7	0.3	34.7

- 579
- 580
- 581
- 582
- 583

Table 2 - Model parameters

$k$	0.1	0.25	0.5	0.75	1
$l_c$ ( $\mu\text{m}$ )	91	41	22	15	11
$\phi_{ref}^{gel}$	0.651	0.263	0.132	0.088	0.066

- 584

585

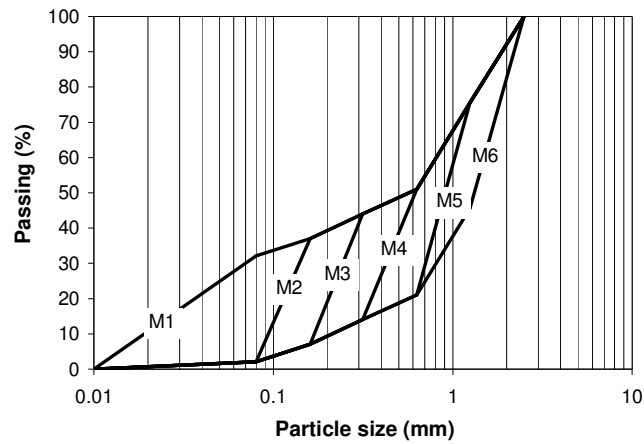


Figure 1 - Particle size distributions of mortars M1 to M6.

586  
587  
588  
589  
590  
591  
592  
593  
594  
595  
596  
597  
598  
599  
600  
601  
602  
603

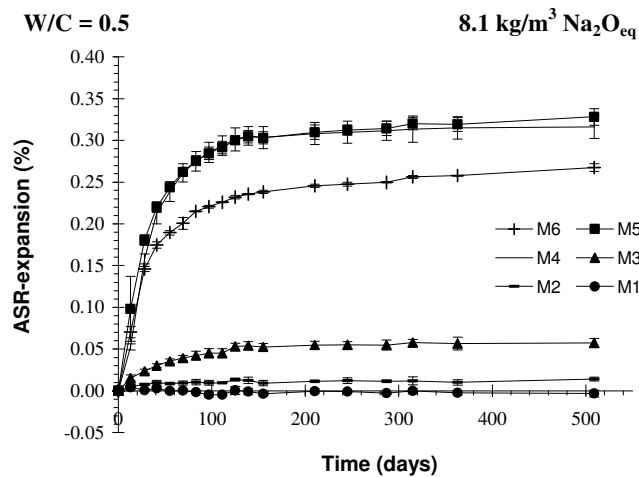
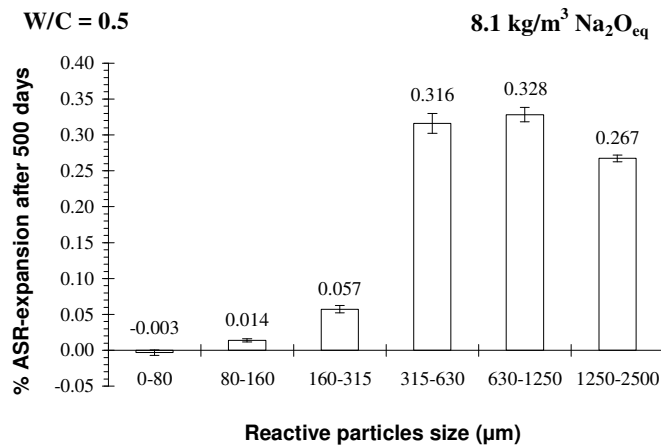


Figure 2 - ASR-expansions of mortars containing 30% of reactive particles of size 0-80 (M1), 80-160 (M2), 160-315 (M3), 315-630 (M4), 630-1250 (M5), 1250-2500  $\mu\text{m}$  (M6) and 70% of continuous 0-2500  $\mu\text{m}$  non-reactive sand.

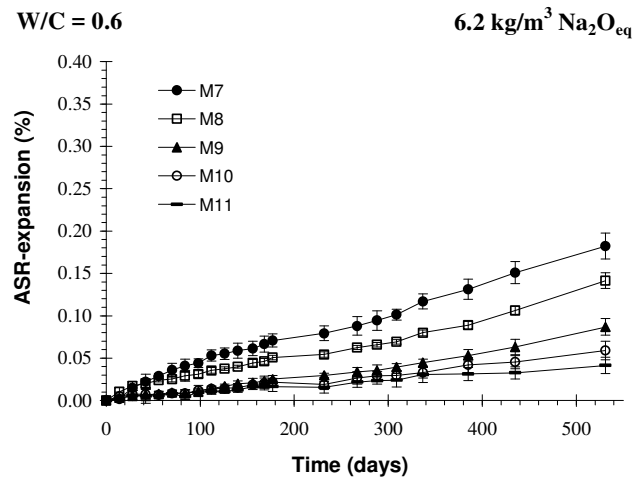
604  
605  
606  
607  
608  
609

610



611  
612  
613  
614  
615  
616  
617  
618  
619  
620  
621  
622  
623  
624  
625  
626  
627  
628

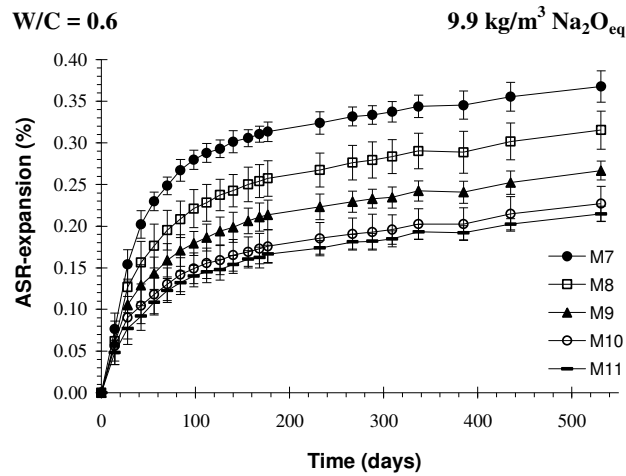
Figure 3 - ASR-expansions of mortars containing 30% of reactive particles of size 0-80 (M1), 80-160 (M2), 160-315 (M3), 315-630 (M4), 630-1250 (M5), 1250-2500 μm (M6) and 70% of continuous 0-2500 μm non-reactive sand after 500 days at 60°C and 95% RH.



629  
630  
631  
632  
633  
634

Figure 4 - ASR-expansions of mortars containing variable proportions of reactive aggregates (mix of reactive particles of two sizes: 0-80 μm and 1250-3150 μm) for 6.2 kg of alkalis per kg of mortar.

635



636

637

638 Figure 5 - ASR-expansions of mortars containing various reactive aggregate contents (mix of  
639 reactive particles of two sizes: 0-80  $\mu\text{m}$  and 1250-3150  $\mu\text{m}$ ) for 9.9 kg of alkalis per kg of  
640 mortar.

641

642

643

644

645

646

647

648

649

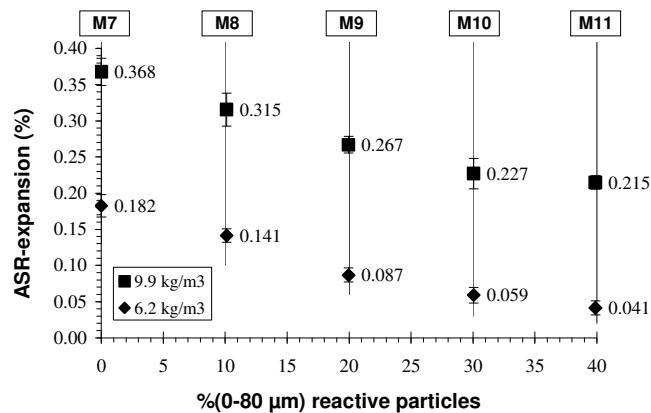
650

651

652

653

654

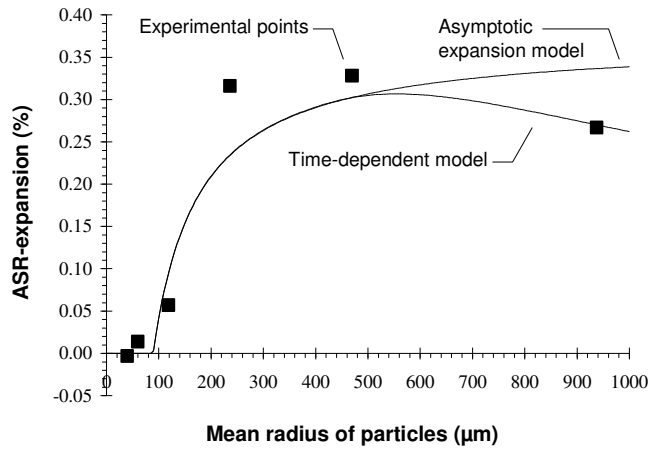


655

656

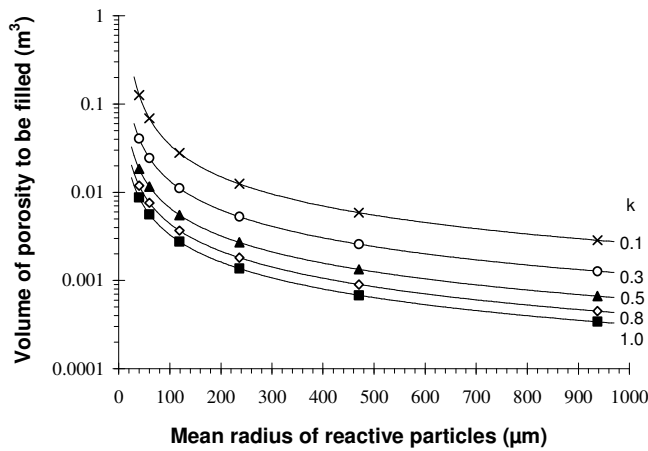
657 Figure 6 - ASR-expansions at 500 days of mortars containing various reactive aggregates  
658 contents (mix of reactive particles of two sizes: 0-80  $\mu\text{m}$  and 1250-3150  $\mu\text{m}$ ) for 6.2 and 9.9  
659 kg of alkalis per kg of mortar. Effect of the amount of fine (0-80  $\mu\text{m}$ ) reactive particles.  
660

661



662  
663  
664  
665  
666  
667  
668  
669  
670  
671  
672  
673  
674  
675  
676  
677  
678  
679

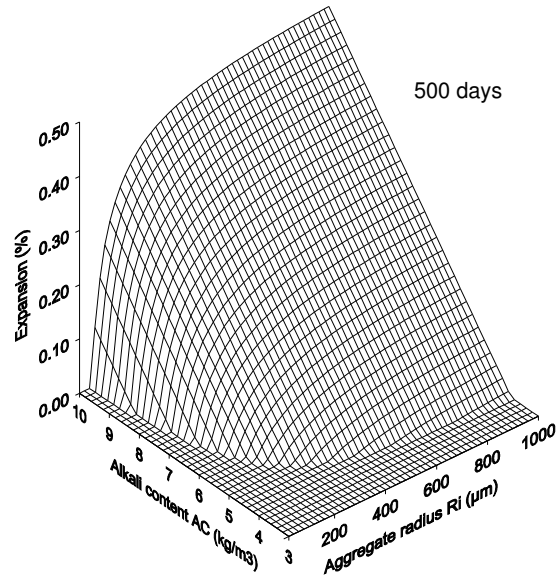
Figure 7 - ASR-expansion of mortars containing one size of reactive particles (M1 to M6) versus mean reactive particle size: comparison between experiments, asymptotic expansion model (section 4.1) and time-dependent model (section 4.2) (*data:  $k$ ,  $l_c$  and  $\phi_{ref}^{sel}$  = any column of Table 2,  $\phi_{void\_mortar}^{void} = 0.17$ ,  $AC_0 = 8.1 \text{ kg/m}^3$ ,  $AC_{th} = 3.5 \text{ kg/m}^3$ ).*)



680  
681  
682  
683  
684

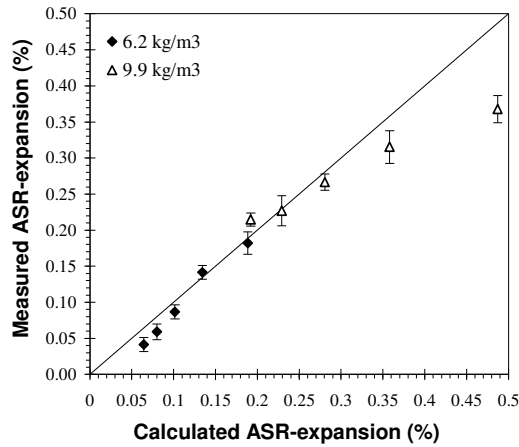
Figure 8 – Volume of porosity to be filled ( $V_i^{poro} \cdot N_i$ , in  $\text{m}^3$  per  $\text{m}^3$  of mortar on a logarithmic scale) when considering the number of reactive aggregate of each size ( $N_i$ )

685



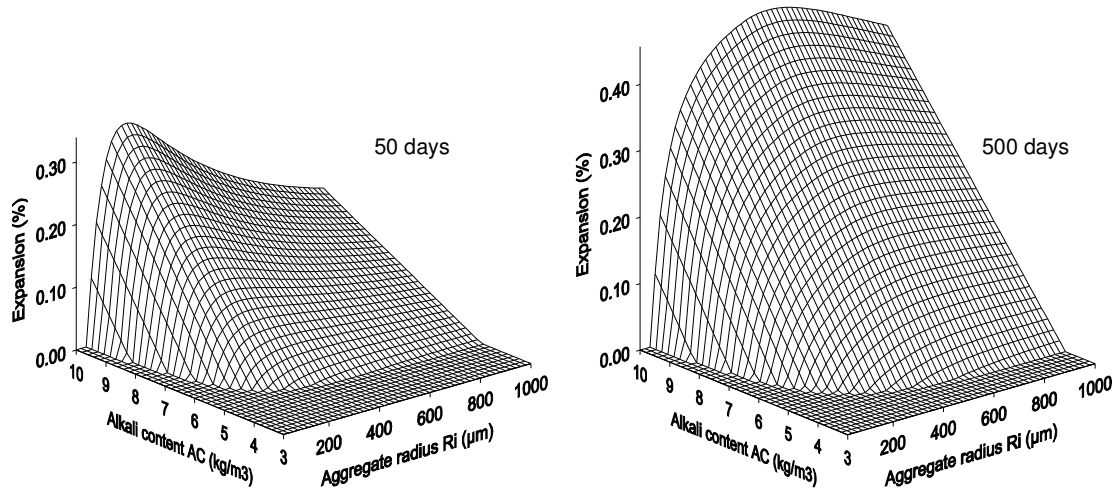
686  
687  
688  
689  
690  
691  
692  
693  
694  
695  
696  
697  
698

Figure 9 - Long-term expansion (t=500 days) versus aggregate radius (R) and initial alkali content (AC) in mortars, calculated using the asymptotic expansion model (*data:  $k=1, l_c=11 \mu\text{m}, \varphi_{ref}^{gel}=0.066, \varphi^{void\_mortar}=0.17, AC_0=8.1 \text{ kg/m}^3, AC_{th}=3.5 \text{ kg/m}^3$* ).



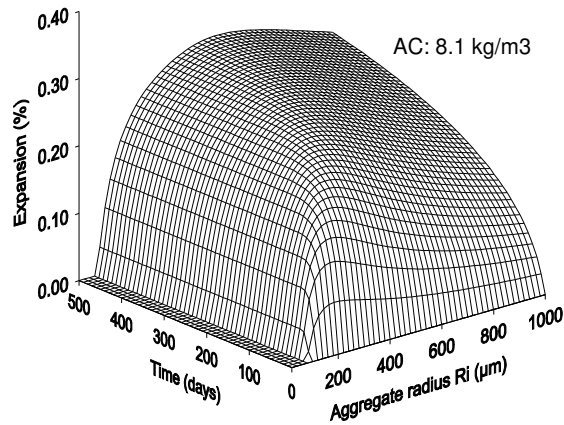
699  
700  
701  
702  
703

Figure 10 - Comparison between the expansions calculated using the asymptotic expansion model and the measured expansions, for mortars containing two sizes of reactive particles.



704  
705  
706  
707  
708  
709  
710  
711  
712  
713  
714  
715  
716  
717  
718  
719  
720

Figure 11 - Expansion versus alkali content (AC) and aggregate size (R) for test durations of 50 and 500 days, calculated using the time-dependent model (*data:  $k=1$ ,  $l_c=11 \mu\text{m}$ ,  $\phi_{ref}^{gel}=0.066$ ,  $\phi^{void\_mortar}=0.17$ ,  $AC_0=8.1 \text{ kg/m}^3$ ,  $AC_{th}=3.5 \text{ kg/m}^3$ ,  $R_{ref}=236 \mu\text{m}$ ,  $t_{ref}=170 \text{ days}$ ).*



721  
722  
723  
724  
725

Figure 12 - Expansion curve simulations for different aggregate diameters, calculated using the time-dependent model (*data:  $k=1$ ,  $l_c=11 \mu\text{m}$ ,  $\phi_{ref}^{gel}=0.066$ ,  $\phi^{void\_mortar}=0.17$ ,  $AC=8.1 \text{ kg/m}^3$ ,  $AC_0=8.1 \text{ kg/m}^3$ ,  $AC_{th}=3.5 \text{ kg/m}^3$ ,  $R_{ref}=236 \mu\text{m}$ ,  $t_{ref}=170 \text{ days}$ ).*